MICROSTRUCTURAL EVOLUTION OF A HIGH CR FE-BASED ODS ALLOY BY DIFFERENT COOLING RATES

YIN ZHONG SHEN, HAE DONG CHO and JINSUNG JANG*
Nuclear Materials Research Center, Korea Atomic Energy Research Institute
1045 Daedeok-daero, Yuseong, Daejeon 305-353, Korea
*Corresponding author. E-mail : jjang@kaeri.re.kr

Received June 15, 2007
Accepted for Publication November 15, 2007

Through mechanical alloying, hot isostatic pressing and hot rolling, a 9%Cr Fe-based oxide dispersion-strengthened alloy sample was fabricated. The tensile strength of the alloy is significantly improved when the microstructure is modified during the post-consolidation process. The alloy samples were strengthened as the cooling rates increased, though the elongation was somewhat reduced. With a cooling rate of 800°C/s after normalization at 1150°C, the alloy sample showed a tensile strength of 1450 MPa, which is about twice that of the hot rolled sample; however, at 600°C the tensile strength dramatically decreased to 620 MPa. Optical microscope and transmission electron microscope were used to investigate the microstructural changes of the specimens. The resultant strengthening of the alloy sample could be mainly attributed to the interstitially dissolved nitrogen, the fraction of the tempered martensite, the fine grain and the presence of a smaller precipitate. The decrease in the tensile strength was mainly caused by the precipitation of vanadium-rich nitride.

KEYWORDS : ODS Alloy, Cooling Rate, Tensile Strength, Microstructure

1. INTRODUCTION

Oxide dispersion-strengthened (ODS) ferritic/martensitic steel is one of the candidate materials for the cladding or in-reactor components of Gen IV reactors, including a supercritical water cooled reactor, due to its improved high temperature mechanical properties and its potentially higher radiation resistance relative to the used base material [1]. The elevated temperature strength in Y_2O_3 ODS steels is obtained through microstructures that contain a high density of small Y_2O_3 particles dispersed in a ferrite matrix; this phenomenon is a result of a dislocation pinning process caused by a dispersion of nano-oxides that originate from the initial Y_2O_3 reinforcements [2-3].

We investigated the microstructural evolution caused by different cooling rates after the normalization treatment of a 9%Cr Fe-based ODS alloy and the effects of the cooling rate on the tensile strength at room temperature and at a high temperature.

2. EXPERIMENTAL PROCEDURE

Our experimental material was a high Cr Fe-based ODS alloy prepared by a mechanical alloying process, hot isostatic pressing (HIP) at 1500°C under 15000 psi, and hot rolling (HR) into plates at 1150°C. Raw metal powders of commercial purity Fe, Cr and V were alloyed with 20 nm to 30 nm of yttria powders. The metal powders were 10 to 20 micron size, except for V, which was less than 45 microns. We then alloyed proportionally mixed powders by using a planetary ball mill in an Ar gas atmosphere. For the milling media, we used steel balls with a diameter of 5 mm. Various ball-to-powder ratios were combined with different milling times from 30 min to 20 h. The chemical composition of the alloy was 9Cr-0.5Y_2O_3-0.5V (in wt%). The hot-rolled alloy samples were normalized at 1150°C for 1 h and cooled at 800°C/s for the water quenching (WQ), 5°C/s for the air cooling (AC), and 0.5oC/s for the furnace cooling (FC). Next we tempered the samples at 750°C for 1 h and then subjected them to air cooling.

Tensile specimens of 1.4 mm $\times$ 3.0 mm $\times$ 15.5 mm were cut from the hot-rolled plate with the tensile axis along the rolling direction. For the tensile tests, we used an Instron-4206 testing machine with an initial strain rate of 5.38×10^{-4} s^{-1} in air. The test temperatures were 25°C and 600°C.

We also took optical micrographs from a sample etched with an etchant of 1g of picric acid, 10 ml of HCl, 10 ml of HNO_3, and 80 ml of ethanol.

Next we prepared extraction carbon replicas by first evaporating carbon on a polished and etched sample

surface of the tensile tested specimens and then dissolving the metallic matrix in a solution of 10%HCl - methanol at 2 V and 20°C.

Thin foil samples were prepared by means of twin-jet electro-polishing in a solution comprising 6% perchloric acid and 35% butyl cellosivle-etchyl alcohol solution at -15˚C with an applied voltage of 35 V. After the tensile tests, we cross-sectioned the thin foil samples of the specimen for the purpose of transmission electron microscope (TEM); this preparation involved nickel plating in an electroplating solution comprising 225g of $NiSO_4$, 100g of $NiCl_2$, 43g of H_3BO_4 and 1000 ml of H_2O followed by ion milling.

The carbon replicas and thin foil samples were examined with the aid of a transmission electron microscope equipped with an energy dispersive X-ray (EDX) spectroscope.

3. RESULTS AND DISCUSSION

Figure 1 shows the stress-strain curves at room temperature of the ODS alloy specimens with different cooling rates after the normalization treatment. As the cooling rate increases, the tensile strengths of the specimens increase with the cooling rate and the elongations decrease. The tensile strength of the WQ specimen is about 1.5 times higher that that of the FC specimen and the elongation is decreased significantly (from 12% to 3.4%).

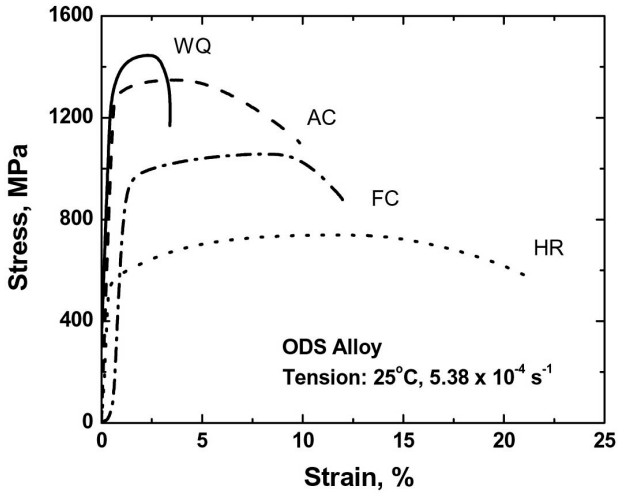

Fig. 1. Stress-Strain Curves at 25°C of the ODS Alloy Specimens with Different Cooling Rates After Normalization Treatment

Figure 2 shows the tensile data of the WQ, AC and HR specimens at 600˚C. The tensile strengths of the WQ and AC specimens decrease to the level of the HR specimen and the elongation of the WQ specimen increases by about 13.6%.

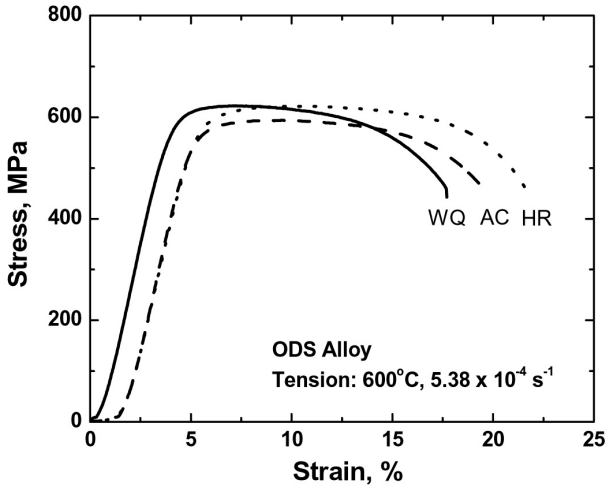

Fig. 2. Stress-Strain Curves at 600°C of the ODS Alloy Specimens with Different Cooling Rates after Normalization Treatment

Figure 3 shows optical micrographs of the ODS alloy samples. The matrix phase with an elongated grain is ferrite. The microstructures indicate that the recrystallization was not complete under the normalization conditions even when a furnace cooling was performed. This result is similar to the results reported by Sakasegawa, et. al. [4].

Figure 4 shows TEM images of the WQ and FC specimens taken from the thin foil samples. Figures 4(a) and 4(d) show an elongated ferrite grain for the WQ and FC specimens. The microstructure of these samples is quite different from the typical martensite structure in the WQ and FC specimens. On the one hand, Figures 4(b) and 4(c) show that the tempered martensite in the WQ specimen has both lath and equiaxed morphologies, though only the equiaxed tempered martensite can be observed in the FC specimen, as shown in Figures 4(e) and 4(f). Note also that the volume fraction of the martensite phase in the WQ specimen is higher than that of the FC specimen. The reason the tensile strength of the WQ specimen is highest during the tensile test at 25˚C is partially due to the higher volume fraction of the tempered martensite in the specimen.

As shown in Figure 3 and Figures 4(a) and 4(d), the elongated ferrite grains remain in the WQ, AC, FC and HR specimens. We can deduce therefore that the difference in the tensile strength of the four specimens, as shown in Figure 1, may not be attributed to the unrecrystallized matrix structures in the alloy specimens.

To estimate the grain size distributions in the alloy specimens with various cooling rates, which are shown in Figure 5, we used electron backscattered diffraction. The grain size was less than 10 μm in the WQ specimen, 20 μm in the AC specimen, and greater than 30 μm in the FC specimen. The average grain size had a diameter of

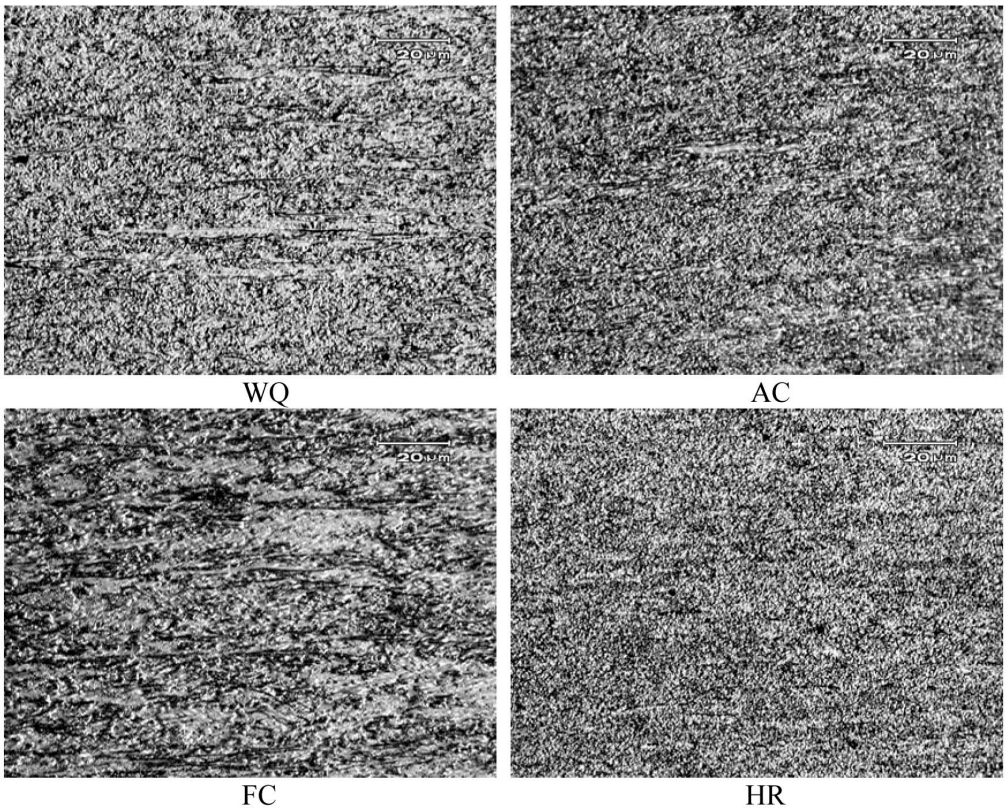

Fig. 3. Optical Micrographs of the ODS Alloy Samples

2.1 microns for the WQ specimen, 4.5 microns for the AC specimen, and 6.4 microns for the FC specimen. Smaller grains at a faster cooling rate could enhance the tensile strength at room temperature.

Oxide particles dispersed in the alloy matrix can also affect the strength at room temperature. We examined the oxide particles in the specimens after the tensile tests at room temperature. Figure 6 shows TEM micrographs at a low magnification of the four specimens taken from the carbon replica samples. Many large Cr-V oxide particles with a diameter range of 0.2 μm to 1 μm were uniformly distributed in the alloy matrix. The chemical composition of the large oxide particles was averaged to be 33.97Cr-8.01V-57.40O-0.48Fe-0.14Y (at%) from the EDX analyses of more than ten large particles.

Figure 7 shows TEM micrographs at a higher magnification of the WQ, AC and FC specimens taken from the thin foil samples. Nano-sized yttrium oxide particles with a diameter in the range of 20 nm to 80 nm were uniformly distributed in the alloy matrix. In general, there is no large difference in the volume fraction, size and distribution of both the large and fine oxide particles in the three tensile specimens. Thus, the striking difference in the tensile strength at 25°C of the alloy specimens with different cooling rates after normalization treatment cannot be attributed to the difference in the nature of the oxide particles in these alloy specimens.

Figure 8 shows a TEM image of the WQ specimen after the tensile test. This image was taken from the carbon replica sample, and the electron microdiffraction patterns were recorded from precipitate particle 1. The microdiffraction patterns, as presented in Figures 8(b), 8(c) and 8(d), completely coincide with the electron diffraction patterns from vanadium nitride (VN, JCPDS file 35-0768) in the three beam directions of [011], [111] and [233], respectively. By combining the EDX analysis from precipitate particle 1, we determined that precipitate 1 was a vanadium-rich nitride phase containing chromium and oxygen with a face-centered cubic (fcc) crystal structure. As shown in Figure 9, some vanadium-rich nitrides with different morphologies are also present in the same replica sample. The chemical compositions of the observed vanadium-rich nitrides, as given in Table 1, were averaged to be about 57V-13Cr-15O-14N (at%).

Because we could not completely prevent the powder from being exposed to air during the milling, degassing or HIP process, the powder could be contaminated by oxygen or nitrogen. A study on the development of ODS alloys indicated that the nitrogen content increases during the compaction process, including the pre-pressing and

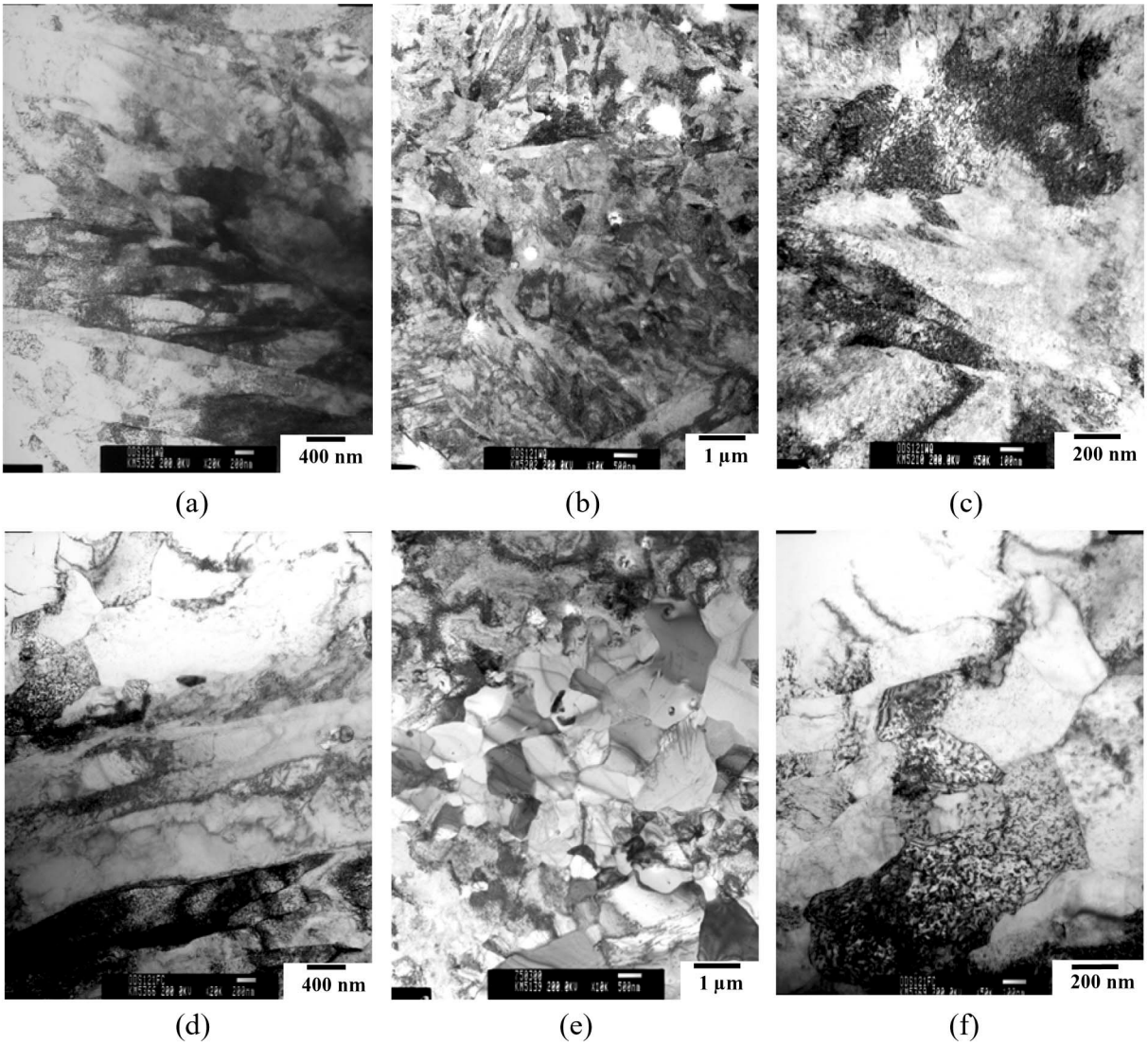

Fig. 4. TEM Images of (a)-(c) the WQ Specimen and (d)-(f) the FC Specimens Taken from Thin Foil Samples

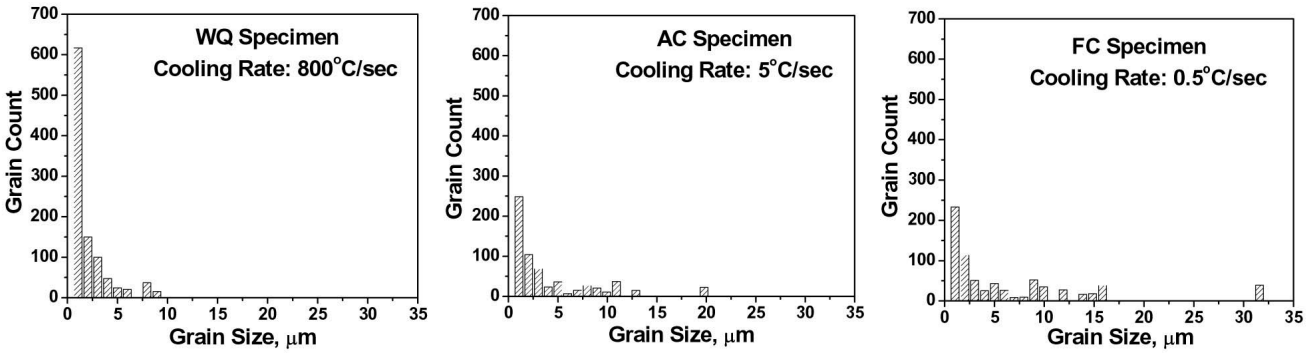

Fig. 5. Grain Size Distribution of the ODS Alloy Specimen with Different Cooling Rates After Normalization Treatment

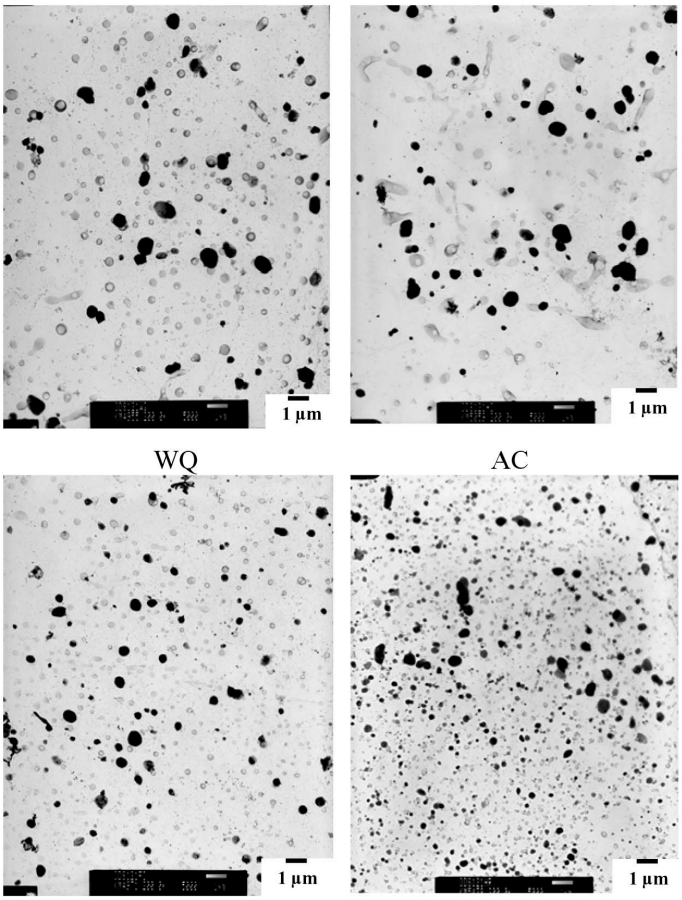

Fig. 6. TEM Micrographs at Low Magnification of Four Specimens Taken from Carbon Replica Samples

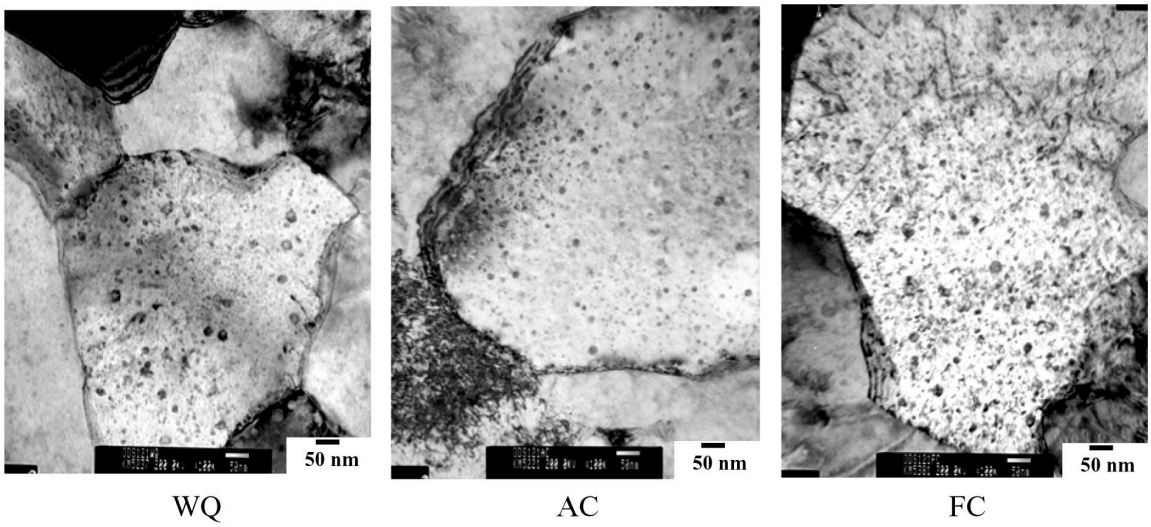

Fig. 7. TEM Micrographs at Higher Magnification of the WQ, AC and FC Specimens Taken from Thin Foil Samples

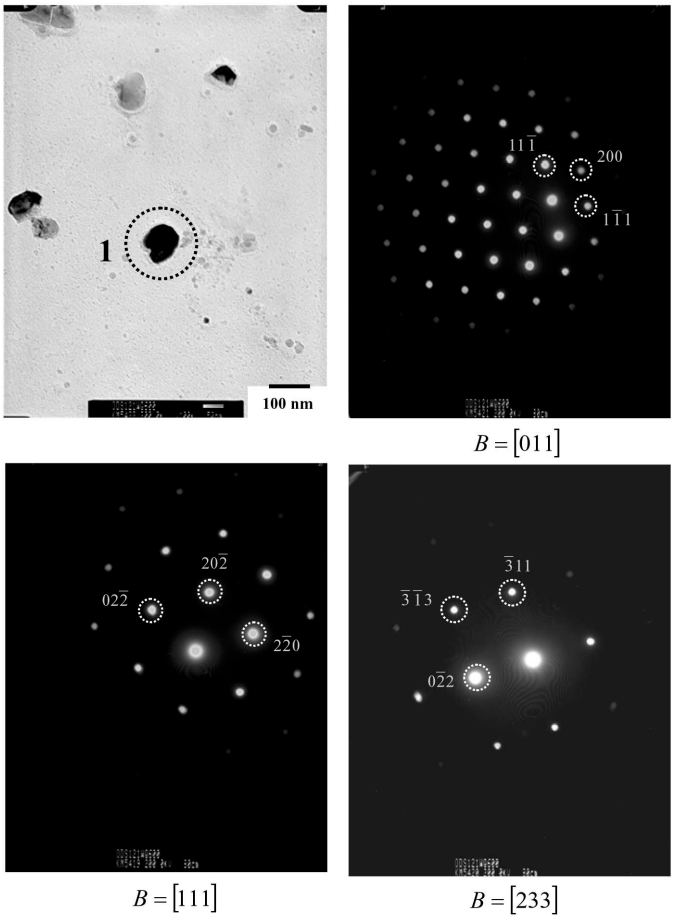

Fig. 8. TEM Image of the WQ Specimen After a Tensile Test at 600ºC Taken from a Carbon Replica Sample and Electron Microdiffraction Patterns Recorded from Precipitate Particle 1

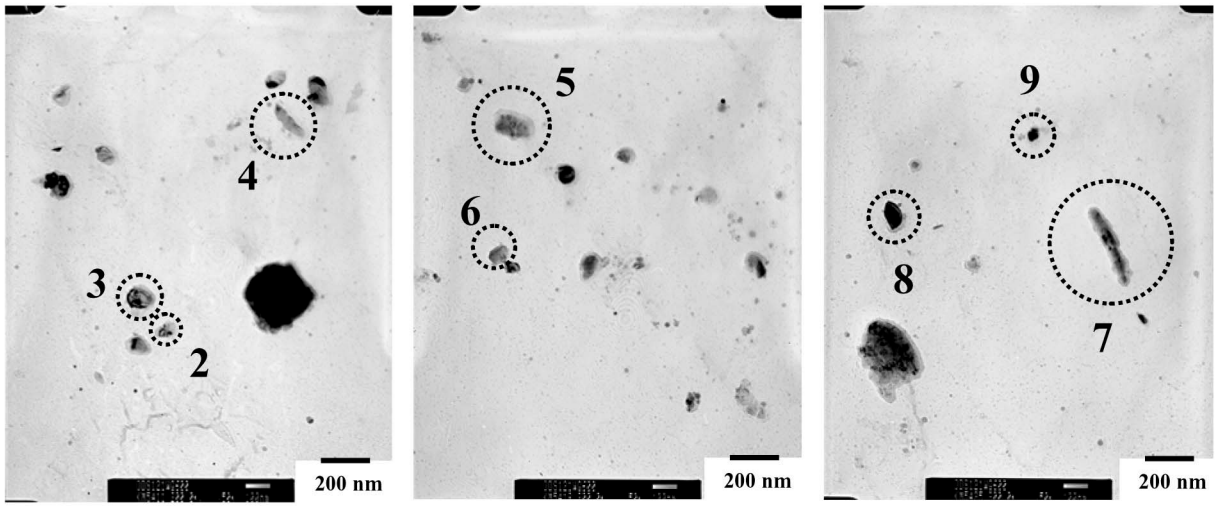

Fig. 9. Micrographs of vanadium-rich nitrides taken from a carbon replica sample of the WQ specimen after a tensile test at 600oC

Table 1. Chemical Composition of the Vanadium-Rich Nitrides in the WQ Specimen After a Tensile Test at 600°C

(at%)

	V	Cr	Fe	Y	O	N
1	61.16	12.92	0.93	0.19	11.75	13.08
2	50.44	10.59	1.43	0.13	20.34	17.08
3	58.48	11.12	0.37	0.17	18.99	10.87
4	52.50	13.30		1.05	16.87	16.27
5	59.06	12.66		1.19	11.64	15.45
6	57.06	15.91	0.28	1.20	11.54	14.01
7	64.31	9.02	0.51	0.33	12.33	13.50
8	64.12	13.67		0.23	9.06	12.93
9	48.65	15.08	1.85	0.42	22.01	11.99
Average	57.31	12.70	0.59	0.54	14.95	13.91

HIP steps [1], and that the alloy matrix contains a lower level of interstitially dissolved impurities (C, N and O) after the process of powder milling or hot pressing [5]. After the normalization treatment at 1150°C for 1 h followed by a water quenching and then a tempering at 750°C, the concentration of the interstitially dissolved nitrogen in the ferrite phase of the alloy specimen must be higher than that in other specimens, leading to a pronounced nitrogen solid-solution-strengthening effect.

One of the strengthening mechanisms of iron and its alloys is known to be solid-solution strengthening by interstitial atoms such as carbon and nitrogen. Dissolved nitrogen is a more effective solid-solution strengthener than carbon at (or below) room temperature in austenitic stainless steels [6-7]. In contrast to austenitic steels, when there is an increase in the concentration of dissolved nitrogen in ferritic steels, the toughness of the steel is diminished. Accordingly, we found that the WQ specimen has higher tensile strength and poor elongation due to the higher concentration of dissolved nitrogen.

According to the Fe-N phase diagram [8], the solubility of nitrogen in γFe is about 8.5at% at 600°C and 9.5 at% at 750°C, whereas the solubility of nitrogen in αFe is about 0.40 at% at 592°C. By assuming that the nitrogen concentration can remain intact in the quenched microstructure, including the martensite and ferrite, we estimate that the nitrogen content in the ferrite after tempering at 750oC is about 3 at% to 9.5 at%. This estimation is based on the EDX analysis, which shows that the average nitrogen concentration of the ferrite in the WQ specimen tempered at 750°C is about 5.07 at%. Super saturated nitrogen in ferrite precipitates to form nitride during a tensile test because the total tension time, including the time to set the specimen and maintain a stable temperature of 600°C is about 1 h. Thus, the temperature and time may be suitable and enough for the precipitation of vanadium nitride in the WQ and AC specimens during tension. Such precipitation leads to a decrease in the concentration of dissolved nitrogen in the ferrite matrix, thereby diminishing the tensile strength of the specimens.

Because the normalization treatment was conducted before the tempering, we expected the dislocation density in the WQ and AC specimens to decrease during the normalization. Thus, the decrease in the tensile strength of the WQ and AC specimens at 600°C could not be attributed to the fact that the dislocation density of the specimens decreases due to the dislocation recovery during the tensile test at 600°C.

4. CONCLUSION

The 9%Cr Fe-based ODS alloy fabricated by means of mechanical alloying, hot isostatic pressing and hot rolling was strengthened as we increased the cooling rates after normalization at 1150°C, though the elongation was reduced to some extent. The TEM results suggest that the strengthening can be mainly attributed to the interstitially dissolved nitrogen, the fraction of tempered martensite, the fine grains, and the smaller size of the precipitate in the alloy specimen. The tensile strength of the WQ specimen decreased dramatically from 1450 MPa at 25°C to 620 MPa at 600°C, mainly due to the precipitation of vanadium-rich nitride.

ACKNOWLEDGEMENT

This study was supported by the Korea Science and Engineering Foundation and the Korean Ministry of Science and Technology through the National Nuclear Technology Development Program.

REFERENCES

[1] R. Schäublin, A. Ramar, N. Baluc, V. de Castro, M. A. Monge, T. Leguey, N. Schmid and C. Bonjour, "Microstructural Development under Irradiation in European ODS Ferritic /Martensitic Steels,"*J. Nucl. Mater*. **351**, 247 (2006).

[2] R. L. Klueh, P. J. Mashimoto, I. S. Kim, L. Heatherly, D. T. Hoelzer, N. Hashimoto, E. A. Kenik and K. Miyahara, "Tensile and Creep Properties of an Oxide Dispersion-strengthened Ferritic Steel," *J. Nucl. Mater*. **307-311**, 773 (2002).

[3] C. Cayron, E. Rath, I. Chu and S. Launois, "Microstructural Evolution of Y_2O_3 and $MgAl_2O_4$ ODS EUROFER Steels during their Elaboration by Mechanical Milling and Hot Isostatic Pressing," *J. Nucl. Mater*. **333**, 83 (2004).

[4] H. Sakasegawa, S, Ohtsuka, S. Ukai, H,Tanigawa, M. Fujiwara, H. Ogiwara and A. Kohyama, "Microstructual Evolution during Creep of 9Cr-ODS Steels," *Fusion Engineering and design* **81**, 1013 (2006).

[5] T. Shibayama, I. Yamagata, H. Kurishita and H. Kayano, "Development of oxide dispersion strengthened vanadium alloy and its properties," *J. Nucl. Mater*. **239**, 162 (1996).

[6] M. L. G. Byrnes, M. Grujicic and W. S. Owen, "Nitrogen strengthening of a stable austenitic stainless steel," *Acta Metall*., **35**, 1853 (1987).

[7] E. Werner, "Solid solution and grain size hardening of nitrogen-alloyed austenitic steels," *Mater Sci Eng* , **A101**, 93 (1988).

[8] H. A. Wriedt, N. A. Gokcen and R. H. Nafziger: *Binary Alloy Phase Diagrams*, **2nd ed**., by T. B. Massalski, H. Okamoto, P. R. Subramanian and L. Kacprzak, ASM, Metals Park, Ohio, 1729 (1990).